



**HAL**  
open science

## Centrifuge study of monopile embedded on its horizontal response in sand

Matthieu Blanc, Luc Thorel, Zhonsen Li

### ► To cite this version:

Matthieu Blanc, Luc Thorel, Zhonsen Li. Centrifuge study of monopile embedded on its horizontal response in sand. ICPMG 2022, 10th International Conference on Physical Modelling in Geotechnics, Sep 2022, Daejeon, South Korea. pp.460-463. hal-04073192

**HAL Id: hal-04073192**

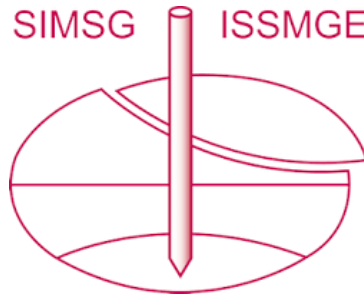
**<https://hal.science/hal-04073192v1>**

Submitted on 18 Apr 2023

**HAL** is a multi-disciplinary open access archive for the deposit and dissemination of scientific research documents, whether they are published or not. The documents may come from teaching and research institutions in France or abroad, or from public or private research centers.

L'archive ouverte pluridisciplinaire **HAL**, est destinée au dépôt et à la diffusion de documents scientifiques de niveau recherche, publiés ou non, émanant des établissements d'enseignement et de recherche français ou étrangers, des laboratoires publics ou privés.

# INTERNATIONAL SOCIETY FOR SOIL MECHANICS AND GEOTECHNICAL ENGINEERING



*This paper was downloaded from the Online Library of the International Society for Soil Mechanics and Geotechnical Engineering (ISSMGE). The library is available here:*

<https://www.issmge.org/publications/online-library>

*This is an open-access database that archives thousands of papers published under the Auspices of the ISSMGE and maintained by the Innovation and Development Committee of ISSMGE.*

*The paper was published in the proceedings of the 10th International Conference on Physical Modelling in Geotechnics and was edited by Moonkyung Chung, Sung-Ryul Kim, Nam-Ryong Kim, Tae-Hyuk Kwon, Heon-Joon Park, Seong-Bae Jo and Jae-Hyun Kim. The conference was held in Daejeon, South Korea from September 19<sup>th</sup> to September 23<sup>rd</sup> 2022.*

## Centrifuge study of monopile embedded length on its horizontal response in sand

M. Blanc & L. Thorel

*Department of Geotechnical Engineering, Environment, Natural Hazards and Earth Sciences, University Gustave Eiffel, France*

Z.S. Li

*Department of Civil Engineering, Aalto University, Finland*

**ABSTRACT:** Model monopiles with outer diameter  $D = 50$  mm are loaded laterally at  $100\times g$  in a large-beam geotechnical centrifuge. To study the effects of the embedded length  $L$  on the lateral response of monopiles, four lengths have been tested:  $L = 150, 250, 350$  and  $450$  mm, corresponding to slenderness ratios of  $L/D = 3, 5, 7$  and  $9$ , respectively. The normal strains on both the tensile and compressive sides are measured using fibre Bragg gratings. Several findings have been observed. The monopiles generate asymmetric tensile and compressive strains during bending. This tension-compression asymmetry is more pronounced at the pile toe and for shorter piles. The piles transition from flexure to rotation as the embedding depth is decreased from  $9D$  to  $3D$ , where the uniqueness of the ground-level rotation and deflection ( $\theta_g - \gamma_g$ ) relationship disappears. Finally, the  $P-y$  curves flattens with increasing embedded depth.

**Keywords:** monopile, centrifuge, embedded length, sand

### 1 INTRODUCTION

A joint academia-industry project, SOLCYP (the French acronym for CYclic SOLicitations on Piles), was started in 2008 with the aim of improving the design methodologies for axially and laterally loaded piles (Puech and Garnier, 2017). In 2017, its extension SOLCYP+ was launched to focus on the lateral responses of monopile foundations for offshore wind turbines (FEM, 2019). As part of the SOLCYP+ project, the present study enriches the database of laterally loaded monopiles.

Since Reese et al. (1974), piles have been designed to take into account horizontal load thanks to soil reaction curves, i.e.  $P-y$  curves. For monopile design, this framework is commonly questioned. Since the slenderness ratio of monopile is very low (under 5 for large monopiles), the beam theory (Euler-Bernoulli or even Timoshenko) may be unsuitable.

The purpose of the study is to study the impact of the embedded length on the horizontal response of monopile. To achieve this goal, monopiles, instrumented with optical fibers, with four different slenderness ratios (from 9 to 3) are tested in the Uni Eiffel's large-beam centrifuge. In this way, monopile axial strains are measured during the horizontal loading. The bending profiles along the monopile depth can be calculated and soil reaction curves obtained from double derivation and double integration. These experimental soil reaction curves, theoretically independent from  $L/D$ , are

compared with each other. In theory, these curves should not depend on the monopile.

### 2 PHYSICAL MODELLING

Tests presented in this study have been performed at acceleration level of 100 times as the earth gravity ( $100\times g$ ) on monopiles scaled by 1:100. The large-beam centrifuge (5.5 m radius), located on the Nantes' campus of the University Gustave Eiffel, is used to minimize acceleration gradient on the embedded length of the monopile.

#### 2.1 Soil model

The model soil is the Fontainebleau NE34 poorly graded sand (Table 1) with a relative density of 81 % obtained by air pluviation into a rectangular strongbox (1200 mm long, 800 mm large and 720 mm high). The final height of the sand mattress is 560 mm.

The strongbox is connected to a water tank by four draining channels at the bottom. The sand mattress is fully saturated and the effective unit weight of  $1.05$  g/cm<sup>3</sup>. The water table is located 30 mm above the ground surface.

Table 1. Characteristics of the Fontainebleau NE34.

Sand	$U_c$ (= $d_{60}/d_{10}$ )	$d_{50}$ ( $\mu\text{m}$ )	$\rho_{d \text{ max}}$ (g/cm <sup>3</sup> )	$\rho_{d \text{ min}}$ (g/cm <sup>3</sup> )
NE34	1.53	210	1.434	1.746

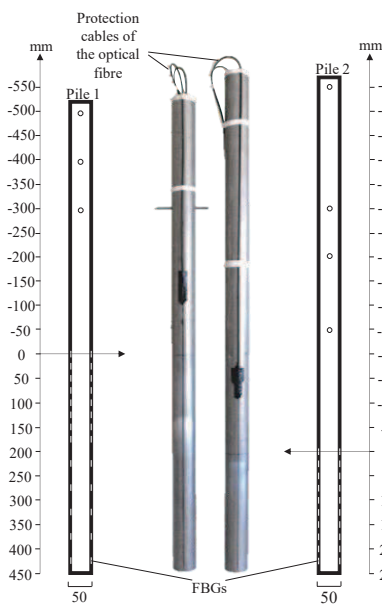


Fig. 1. Geometry of the instrumented model monopiles.

## 2.2 Monopile model

Two monopiles have been considered: “pile 1” for test with  $L/D = 9$  and 7; “pile 2” for tests with  $L/D = 5$  and 3 (Figure 1). These monopile models are aluminum 2017A tubes, with a Young modulus  $E = 72.5$  MPa and a plasticity limit  $\sigma_p = 280$  MPa. Their model dimensions are: the external diameter  $D = 50$  mm, the internal diameter  $d = 45$  mm so the wall thickness more 200 times higher than the medium sand grain diameter  $d_{50}$ .

For each monopile, two identical optical fibers are glued in two grooves (Li et al, 2020). Depending on the monopile length, 10 or 13 Fiber Bragg Grating sensors (FBGs) have been manufactured until 250 mm of 450 mm from the pile base. These FBGs measure the external axial strains at 10 or 13 different cross sections and then, after calibration, give the bending moments at the corresponding depths (Figure 2).

## 2.3 Set-up

With a hydraulic jack, the monopile is installed at  $1 \times g$  at a constant rate 1 mm/s. At the end of the installation, the sand level inside the pile is checked and there is no plug generated. In this way, this installation method models a wished-in-place pile.

An electric actuator with 150 mm stroke is placed above the strongbox (Figure 3). At the actuator termination, a fork is screwed in the load sensor. This fork pushes the rod that crosses the monopile and apply the lateral load in the middle of the cross section, which is 500 mm above the ground level (i.e.  $10D$ ). The actuator is displacement controlled at 0.1 mm/s in model scale.

To measure the horizontal displacement of the monopile above the ground surface, four laser

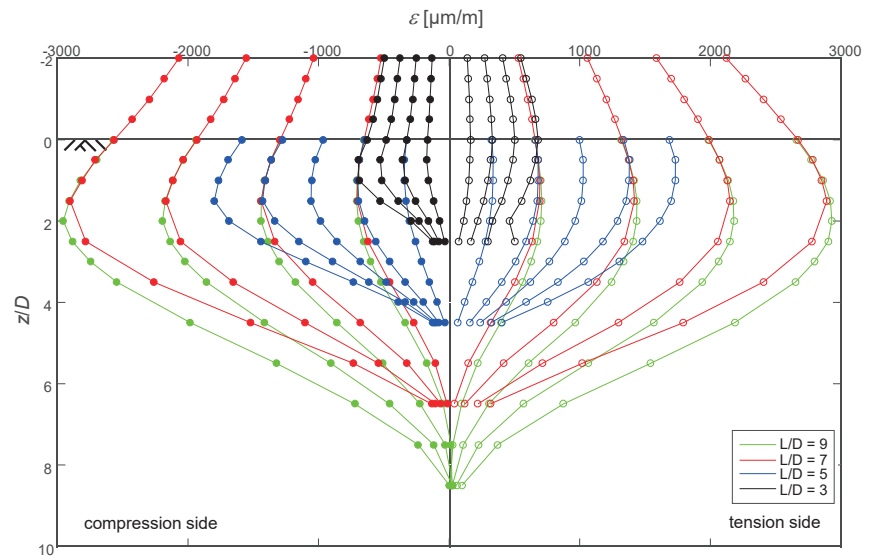


Fig. 2. Axial strain measurements for  $L/D = 3, 5, 7$  and 9.

displacement transducers are positioned in front of the monopile at 40 mm, 210 mm, 410 mm and 610 mm above the ground surface.

## 3 RESULTS & DISCUSSION

Four tests with different  $L/D = 9, 7, 5$  and 3 are performed with the same load eccentricity  $L_e/D = 10$ .

### 3.1 Global behaviour at ground level

In Figure 3, are respectively plotted, at ground level, the moment  $M_g$  versus the rotation  $\theta_g$  and the rotation  $\theta_g$  versus the lateral displacement  $y_g$ . For a given  $y_g$  or  $\theta_g$ , the moment and horizontal load increase with the slenderness ratio. The key feature is the relationship between  $y_g$  and  $\theta_g$ . For high slenderness

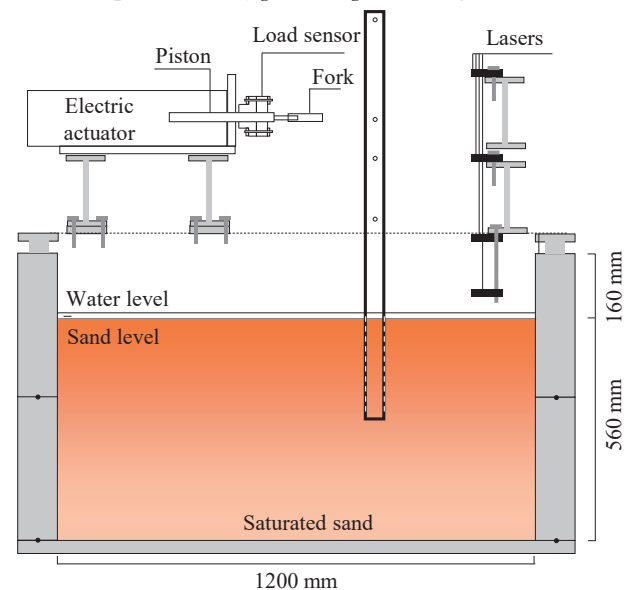


Fig. 3. Schema of the lateral loading and measuring systems.

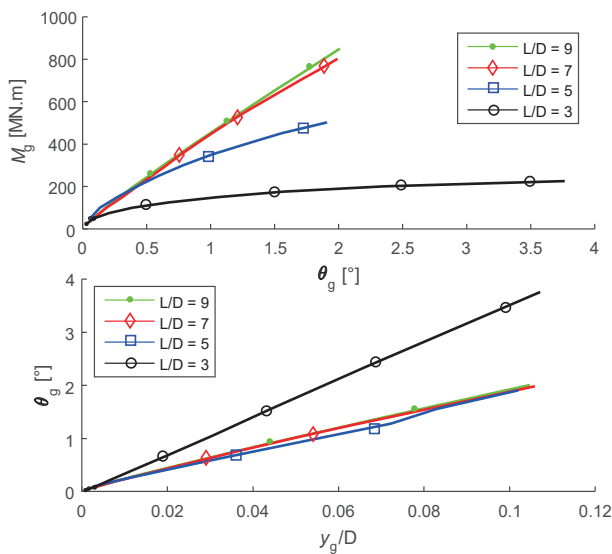


Fig. 4. Monopile behaviour at ground level.

ratios (above 5), this relationship is unique. However, for the smallest slenderness ratio ( $L/D = 3$ ), there is much more rotation than horizontal displacement. This observation shows that the pile behaviour changes for slenderness ratios between 3 and 5. The hypotheses of the beam theory appear to be inappropriate for this short pile.

### 3.2 Monopile axial deformation

Figure 2 presents the strains measured by the FBGs along the depth for  $L/D = 3, 5, 7$  and  $9$ . These results show different behaviours in the compression side than in the tension. In the first half part of the pile, there is more compression strains than tension strains, whereas in the second half, the situation is opposite – tensile strains are more prominent than the compressive strains.

The difference becomes larger as the slenderness ratio decreases. For  $L/D = 9$ , there is nearly no difference, showing that the difference (i.e. tension-compression asymmetry) is not due to the instrumentation or the set-up but a real behaviour of the monopile. For low slenderness ratios, a difference between the compression side and the tension one appears.

Similar observations were also noticed in field tests on University College Dublin dense sand (Doherty et al., 2015) and Dunkirk marine dense sand (McAdam et al., 2020). In the superficial layer below the ground, the pile deflection induces constraints from the soil (passive earth pressure) that in return prevent the pile lateral displacement. The large constraints on the pile front enhance the soil-pile contact and increase the tangential and friction stresses. Consequently, the strains on the pile front (i.e. compressive strains) increase and may become larger than the tensile strains, such as for  $L/D = 3$  and  $5$ . In the deeper layers, the tensile strains are always larger than the compressive one; this is due to the combined effects of larger (i) constraints (passive earth pressure or soil reaction), (ii) shaft friction and (iii) base shear on the negative mobilization zone.

### 3.3 Monopile local behaviour

With monopile mechanical properties, the bending moments are calculated at the FBGs levels. For several loads, these bending moments  $M$  along the monopile depth  $z$  are fitted with a cubic smooth splines function. The soil reaction profile  $P$  is obtained by a second order differential operation. The pile rotation angle  $\theta$  and deflection  $y$  are obtained by solving first and second-order integrals. For this purpose, two integration constants are required: (i) the pile deflection measured by the laser sensors and (ii) the pivot point based on the

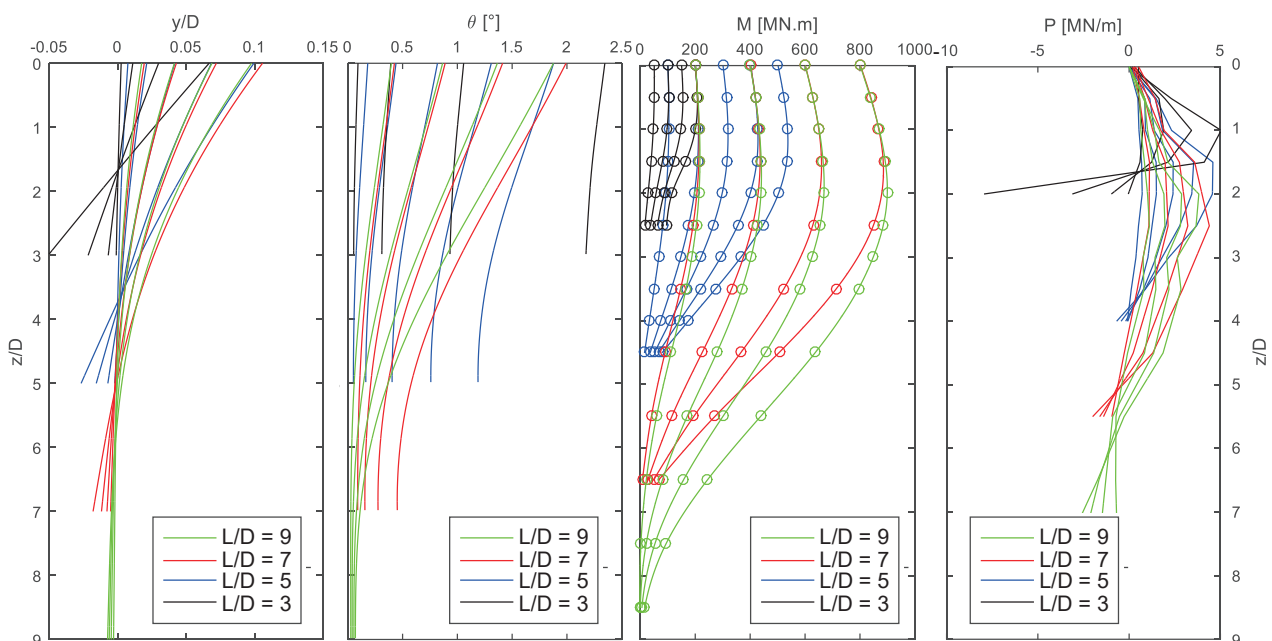


Fig. 5. Pile deflection  $y$ , rotation angle  $\theta$ , bending moment  $M$  and soil reaction  $P$  versus depth  $z$  for  $L/D = 3, 5, 7$  and  $9$ .

analysis of the soil reaction developed in Li et al. (2022).

Figure 5 (from left to right) presents the profiles of pile deflection  $y$ , rotation angle  $\theta$ , bending moment  $M$  and soil reaction  $P$ . At the pile toe, as  $L/D$  is increased from 3 to 9, the deflection and rotation angle decrease to null even though the applied bending moments are larger. At  $L/D = 3$ , the profiles of the pile deflection can be deemed as a series of straight lines, meaning that the pile only rotates and there is practically no flexure. At  $L/D = 9$ , the deflection at depths of 7–9D is almost null, indicating a strong embedding force and negligible rotation. For the values of  $L/D$  in between, one may notice a series of curved lines with nonzero values at the pile end, which in fact suggests a combination of rotation and flexure. In the present study, the pile behaviour undergoes a clear transition (i.e. from rigid rotation to pure flexure) as the generalised embedding depth  $L/D$  is increased from 3 to 9.

### 3.3 Soil reaction curves

Figure 6 shows the relationship between the soil reaction  $P$  and the normalised deflection  $y/D$  at  $z = D$ . The  $P$ - $y/D$  curves tend to be steeper when the slenderness ratio is decreased from 9 to 3. This seems unusual given that the soil stiffness is constant and its stress-strain relationship should be unique at a given depth. One possible reason of the steepening  $P$ - $y/D$  curve is that Euler-Bernoulli beam theory underestimates the lateral deflection of short piles. Nevertheless, one should be cautious when analysing these results from centrifuge tests. The second reason is that the distributed moment generated by differential shaft friction has not been considered in this study. As introduced in the PISA project by Byrne et al. (2017), this distributed moment has to be considered to design short monopiles. However, experimentally, it is impossible to evaluate this distributed moment by FBGs.

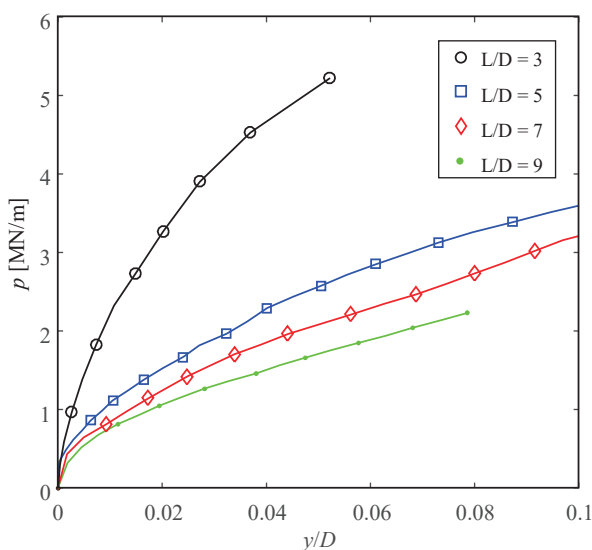


Fig. 6. Soil reaction curve for  $z = 1D$ .

Only the total bending moment can be calculated from FBGs measurements. Then, in this study,  $P$ - $y/D$  curves are not only due to the horizontal soil reaction but also to the distributed bending moment along the monopile shaft.

## 4 CONCLUSIONS

Four centrifuge tests have been performed on a model pile that instrumented with FBGs. The effect of embedded length is investigated by loading the pile at  $L/D = 9, 7, 5$  and 3. The monopile shows different behaviours at different slenderness ratio. For  $L/D > 7$ , the monopile can be considered as slender and flexible. For  $L/D = 3$ , the monopile is a rigid body and the  $P$ - $y/D$  curves, generated using classical framework for slender pile, lead to an overestimation of the horizontal soil reaction. The transition between these two different behaviours is between  $3 < L/D < 5$ .

## ACKNOWLEDGEMENTS

This work received state support managed by the National Research Agency under the Investments for the Future Program (ANR-10-IEED-0006-08, SOLCYP+) and financial support from France Energies Marines (2017). The technical staff at the centrifuge group of Gustave Eiffel University helped in building up the experimental devices, they are greatly acknowledged.

## REFERENCES

- Byrne, B.W., McAdam, R.A., Burd, H.J. et al. 2017. PISA: New design methods for offshore wind turbine monopiles. Proc. 8th Int. Conf. on Offshore Site Investigation and Geotechnics, London, Vol 1, 142-161.
- Doherty, P., Igoe, D., Murphy, G. et al. (2015). Field validation of fibre Bragg grating sensors for measuring strain on driven steel piles. *Geotechnique Letters*, (5)2, 74-79.
- Doherty, P., Igoe, D., Murphy, G. et al. 2015. Field validation of fibre Bragg grating sensors for measuring strain on driven steel piles. *Geotechnique Letters*, (5)2, 74-79.
- France Energies Marines 2017. <https://en.france-energies-marines.org/R-D/Projects-in-progress/SOLCYP> (Accessed on December 8th, 2021).
- Li, Z. S., Blanc, M. & Thorel, L. 2020. Using FBGS to estimate the horizontal response of a monopile in a geotechnical centrifuge. *International Journal of Physical Modelling in Geotechnics*, 20(3), 164-174.
- Li, Z. S., Blanc, M. & Thorel, L. 2022. Effects of embedding depth and load eccentricity on lateral response of offshore monopiles in dense sand: A centrifuge study. *Geotechnique*. (10.1680/jgeot.21.00200)
- McAdam, R.A., Byrne, B.W., Houlsby, G.T. et al. 2020. Monotonic laterally loaded pile testing in a dense marine sand at Dunkirk. *Geotechnique*, 70(11), 986-998.
- Puech, A. & Garnier, J. 2017. Design of piles under cyclic loading: SOLCYP recommendations. London: ISTE - Wiley.
- Reese, L.C., Cox, W.R., & Koop, F.D. 1974. Analysis of laterally loaded piles in sand. *In Offshore Technology Conference*.